## TITLE

*In vitro* models for liver organogenesis and synthetic tissues including assembloid formation and multiple modes of collective migration


## AUTHORS AND AFFILIATIONS:

Simran Kumar[1], Jenna Venturo[1], Helly Patel[1], Natesh Parashurama[1,2,3,4,5]

[1] Department of Biomedical Engineering, University at Buffalo (State University of New York), Furnas Hall, Buffalo, NY 14260
[2] Clinical and Translation Research Center (CTRC), University at Buffalo (State University of New York), 875 Ellicott St., Buffalo, NY 14203
[3] Department of Chemical and Biological Engineering, University at Buffalo (State University of New York), Furnas Hall, Buffalo, NY 14260
[4] Center for Cell, Gene and Tissue Engineering, University at Buffalo, State University of New York, Furnas Hall Buffalo NY 14260
[5] Khufu Therapeutics, Inc. Buffalo, NY, 14260

**Corresponding Author:**
Natesh Parashurama, 906 Furnas Hall, Buffalo, NY 14260; Tel: 716-645-1201; Fax: 716-645-3822; e-mail: nateshp@buffalo.edu



## KEYWORDS:

organogenesis, liver development, collective cell migration, epithelial to mesenchymal transition, liver diverticulum, liver bud



## SUMMARY:

Organoids revolutionize personalized tissue modeling for organ development, drug discovery, and disease research. Organoid engineering extends this to create more extensive synthetic tissues. We aim to merge morphogenesis, assembloid technology, and biomatrices to advance tissue engineering. Our methods aid in modeling liver organogenesis and establishing guidelines for synthetic tissue construction.

## ABSTRACT:

Chronic liver disease has reached epidemic proportions, affecting over 800 million people globally. The current treatment, orthotopic liver transplantation, has several limitations. Promising solutions have emerged in the field of liver regenerative medicine, with liver organogenesis holding significant potential. Early liver organogenesis, occurring between E8.5 and 11.5, involves the formation of epithelial-mesenchymal interactions leading to morphogenesis, hepatic cord formation, and collective migration. However, there is a lack of methods for in vitro modeling of this process. In this study, we present a detailed series of methods enabling the modeling of various stages and aspects of liver organogenesis. In one method series, we utilize assembloid technology with hepatic and mesenchymal spheroids, which replicate early structures found in liver organogenesis, model early morphogenesis, and demonstrate interstitial cell migration as seen in vivo. These innovative assembloid systems help identify factors influencing assembloid formation and migration. Hepatic spheroid cultivation systems were also employed to model collective

migration and branching morphogenesis. Fibroblast-conditioned media play a significant role in initiating dose-dependent branching migration. Future work will involve high temporal and spatial resolution imaging of hepatic and mesenchymal interactions to determine the cascade of cellular and molecular events involved in tissue formation, morphogenesis, and migration.

## INTRODUCTION:

Liver cell migration plays a significant role in liver organogenesis, disease, and cell therapy. During liver organogenesis (E8.5-9.0, mouse), the ventral foregut pre-hepatic epithelium begins to express liver genes, due to the inductive signals emanating from the surrounding mesenchyme and heart. At E9.0, the foregut epithelium thickens as the cells transition from a cuboidal to a pseudostratified columnar morphology, to form the liver diverticulum (**Gualdi, Bossard et al. 1996**); (**Bort, Signore et al. 2006**). At this critical stage, the liver diverticulum is comprised of only ~1,500 cells. Next, the hepatic endoderm lining the liver diverticulum thickens, delaminates, and forms cords of hepatoblasts that co-migrate with endothelial cells and mesenchymal cells and branch into the surrounding mesenchymal tissue, thus initiating three-dimensional collective cell migration to form the liver bud (**Ogoke, Oluwole et al. 2017**); (**Ogoke O. 2022**). In fact, during this stage, the cells collectively undergo; 1) co-migration, or movement together with other cell types, 2) branching morphogenesis or formation of branching tube-like structures, and, 3) interstitial migration, or migration on top of other cells. By E11.5, migration ceases, the primitive liver has formed and has expanded $10^3$-fold (**Ogoke O. 2022**). Liver cell migration may also be required in later stages of liver organogenesis, as rat fetal hepatoblasts (HBs) expression have shown evidence of highly upregulated genes associated with 3D collective cell migration, morphogenesis, and extracellular matrix remodeling **(Petkov, Kim et al. 2000**). In addition to its role in early liver organogenesis, 3D collective migration is intricately linked to the local spread and metastasis of advanced hepatocellular carcinoma (HCC), ultimately leading to worsened prognosis and increased treatment resistance **(Yang, Chen et al. 2009**). Adult and fetal hepatocytes also employ collective migration when moving from the spleen to within the liver during liver repopulation; *in vivo* imaging studies have demonstrated that transplanted hepatocytes enter the portal vein and then the capillaries within hours, migrate across the liver sinusoids, and through the liver tissue (**Rajvanshi, Kerr et al. 1996**);(**Gupta, Rajvanshi et al. 1999**);(**Koenig, Stoesser et al. 2005**). Finally, recent studies demonstrate that migrating hepatoblasts arise during murine and human liver regeneration with some evidence of movement in sheets (**Matchett KP 2023**). Overall, liver collective migration, capable of multiple modes of morphogenesis, plays a significant role in organogenesis, cancer, hepatocyte cell therapy, and liver regeneration.

Numerous genetic studies have investigated the molecular pathways that drive 3D liver collective cell migration. These studies demonstrate that ablation of the hepatic cords blocks liver formation and demonstrates that therefore, formation of hepatic cords and their ensuing interactions with supporting cells are required for liver formation (**Bort, Signore et al. 2006**); (**Suzuki, Sekiya et al. 2008**); (**Sosa-Pineda, Wigle et al. 2000, Matsumoto, Yoshitomi et al. 2001**). These studies also demonstrate that liver growth is initiated by fibroblast growth factor 2 (FGF2) secreted from the cardiac mesoderm, BMP4

secreted from the surrounding mesenchyme, HGF, endothelial cell interactions, and migration-associated transcription factors including HEX, PROX1, and TBX3 (**Gualdi, Bossard et al. 1996**); (**Rossi, Dunn et al. 2001**). Overall, genetic studies support the fact that soluble factor signaling with transcription factor expression is responsible for driving migration, signaling, and molecular interactions between hepatoblasts and their surrounding mesenchyme.

Although cell migration in early liver organogenesis has been extensively investigated, the current *in vitro* hepatic migration studies frequently utilize 2D assays consisting of highly migratory HCC cells combined with *in vivo* tumor models (**Ng, Tung-Ping Poon et al. 2013**). These studies have provided insight into several factors that play a role in hepatic migration including TGFB1 **(Fransvea, Angelotti et al. 2008**) c-Myc (**Zhao, Jian et al. 2013**), Yes associate protein (YAP) (**Fitamant, Kottakis et al. 2015**), goosecoid (**Xue, Ge et al. 2014**), actopaxin (**Binamé, Lassus et al. 2008**), and miRNAs **(Zeng, Liang et al. 2016**);(**Chen, Liang et al. 2017**);(**Yang, Xu et al. 2017**). Despite the advancements in understanding the molecular mechanisms in 3D hepatic cell migration, the fundamental mechanisms between 2D and 3D cellular migration are distinct which suggests 2D assays have their limitations. Furthermore, these models typically do not implement mesenchymal cell types, which are essential to migration/growth. There has been progress in the development of 3D models for liver migration that incorporate the supporting mesenchyme, however, they are solely focused on co-migration rather than the different modes of collective migration.

The ability to form tissues from spheroids through various self-assembly and morphogenetic processes enables the scientific study of synthetic tissues for applications for drug development and screening, disease modeling, therapy, and other biomedical and biotechnological applications. Here we present methodological details for several 3D *in vitro* cultivation systems which were engineered to exhibit different modes of liver 3D collective migration. These systems include the following: (1) co-spheroid culture with hepatic and mesenchymal-derived spheroids in matrix, (2) spheroid matrix droplet cultured with fibroblast conditioned medium, and (3) mixed spheroids (hepatic and mesenchymal-derived cells). These systems enable robust modeling of liver 3D collective migration which will improve our molecular and cellular understanding of liver organogenesis, cancer, and therapy.

## PROTOCOL:

### 1. Preparation of 1% Low EEO Agarose Solution

1.1. Measure 2.5 g of agarose powder (low EEO) and transfer it to a beaker.

NOTE: The beaker should be at least twice the size of the desired volume to account for the bubbling of the solution.

1.2. Use a graduated cylinder to measure 250 mL of distilled water (DI) water and transfer it to the beaker to dilute the agarose to obtain a final concentration of 1%.

1.3. Cover the mouth of the beaker with plastic wrap and make a small hole. Heat the beaker in the microwave.

1.4. After 30 seconds, remove the beaker and swirl until uniform. Repeat every 30 seconds, until the agarose completely dissolves.

CAUTION: Microwaved glassware should be handled very carefully by wearing proper gloves. The solution should be watched closely to avoid overheating or boiling over.

1.5. Remove the beaker from the microwave and gently swirl. Transfer the solution to a pre-sterilized bottle and autoclave the solution. Store the agarose solution at room temperature until ready to use.

## 2. Coating 96-Well Plate

2.1. Loosen the cap of the bottle containing the 1% agarose solution. Warm the solution in the microwave until the solution is in the liquid phase and tighten the cap.

CAUTION: Microwaved glassware should be handled very carefully by wearing proper gloves. The solution should be watched closely to avoid overheating or boiling over.

NOTE: Perform these steps under a sterile tissue culture laminar flow hood.

2.2. Use 55-65 µL of the sterile 1% agarose solution per well to coat the 96-well tissue cultured plate and immediately rotate the plate.

2.3. Once the 1% agarose solution has been transferred to the desired number of wells, allow the agarose to solidify by allowing the plates to cool for 20-30 minutes in a 4℃ fridge. Prior to use, bring the plate to room temperature (**Figure 1A**).

## 3. Preparation of HepG2-WT Spheroids

3.1. Cultivate HepG2-WT cells in a T-75 flask with completed growth medium (cDMEM) containing Dulbecco's Modified Eagle Medium (DMEM), supplemented with 10% Fetal Bovine Serum (FBS) and 1% Penicillin-Streptomycin (Pen-Strep). Incubate the cell culture at 37℃ and 5% $CO_2$ with medium changes every day.

3.2. Once the cell culture reaches 80% confluency, add 0.05% of Trypsin-EDTA to the flask for 5-10 minutes. Add equal amounts of cDMEM and wash the cells off the flask.

3.3. Once the cells have detached, transfer the mixture to a 15 mL sterile conical centrifuge tube and centrifuge the cell suspension at 300 *x g* for 5 minutes.

3.4. Re-suspend the cell pellet in sterile 1X Phosphate Buffered Saline (PBS) and centrifuge the cell suspension at 300 *x g* for 5 minutes.

3.5. Based on the cell count, suspend the cell suspension to obtain a final concentration of 1x $10^6$ cells/mL (**Figure 1B**).

3.6. Dye-labeling of cells

NOTE: This is an optional step.

3.6.1. Transfer the desired amount of cell suspension to a 15 mL sterile conical centrifuge tube and centrifuge the cell suspension at 300 *x g* for 3 minutes.

3.6.2. Re-suspend the cell pellet in a serum-free growth medium to obtain a final concentration of 1 x $10^6$ cells/mL. Add 5 µL of Vybrant Cell-Labeling Solution per mL of cell suspension and incubate the cell suspension on rotation for 20 minutes, preferably at 37°C.

NOTE: Serum-free growth medium is DMEM only supplemented with 1% Pen-strep. Different densities of the cell suspension may require longer incubation time for uniform staining.

3.6.3. Once the incubation is completed, centrifuge the cell suspension at 450 *x g* for 5 minutes and resuspend the cell pellet in fresh cDMEM. Repeat this wash process two more times (**Figure 1C**).

3.7. Spheroid formation

3.7.1. Suspend the cells in fresh cDMEM to obtain a final concentration of 5.0 x $10^4$ cells/mL. Mix the cell suspension very well and transfer 100 µL of cell suspension per well to the agarose-coated 96-well plate.

NOTE: The density of cell suspension is to obtain a density of 5,000 cells per well in the agarose-coated 96-well plate.

3.7.2. Centrifuge the plate at 340 *x g* for 10 minutes and incubate at 5% $CO_2$ at 37°C for 5-9 days (**Figure 1D**).

NOTE: Change medium every other day after plating with gentle removal of 50% of cDMEM and replacement.

NOTE: HepG2-WT spheroids can be used for the HEP-MES assembloid model or M-CM model.

## 4. Preparation of HFF/MRC-5 Spheroids

4.1. Cultivate HFF/MRC-5 cells in a T-175 flask with completed growth medium (cDMEM) containing Dulbecco's Modified Eagle Medium (DMEM), supplemented with 10% Fetal Bovine Serum (FBS) and 1% Penicillin-Streptomycin (Pen-Strep). Incubate the cell culture at 37℃ and 5% $CO_2$ with medium changes every other day.

4.2. Once the cell culture reaches 80% confluency, add 5 mL of 0.25% of Trypsin-EDTA to the flask for 5-10 minutes. Add equal amounts of cDMEM and wash the cells off the flask.

4.3. Once the cells have detached, transfer the mixture to a 15 mL sterile conical centrifuge tube and centrifuge the cell suspension at 300 *x g* for 3 minutes.

4.4. Re-suspend the cell pellet in sterile 1X Phosphate Buffered Saline (PBS) and centrifuge the cell suspension at 300 *x g* for 3 minutes.

4.5. Based on the cell count, suspend the cell suspension to obtain a final concentration of 1x $10^6$ cells/mL (**Figure 1B**).

4.6. Dye-labeling of Cells

NOTE: This is an optional step.

4.6.1. Transfer the desired amount of cell suspension to a 15 mL sterile conical centrifuge tube and centrifuge the cell suspension at 300 *x g* for 3 minutes.

4.6.2. Re-suspend the cell pellet in a serum-free growth medium to obtain a final concentration of 1 x $10^6$ cells/mL. Add 5 µL of Vybrant Cell-Labeling Solution per mL of cell suspension and incubate the cell suspension on rotation for 20 minutes, preferably at 37°C.

NOTE: Serum-free growth medium is DMEM only supplemented with 1% Pen-strep. Different densities of the cell suspension may require longer incubation time for uniform staining.

4.6.3. Once the incubation is completed, centrifuge the cell suspension at 450 *x g* for 5 minutes and resuspend the cell pellet in fresh cDMEM. Repeat this wash process two more times (**Figure 1C**).

4.7. Spheroid Formation

4.7.1. Suspend the cells in fresh cDMEM to obtain a final concentration of 5.0 x $10^4$ cells/mL. Mix the cell suspension very well and transfer 100 µL of cell suspension per well to the agarose-coated 96-well plate.

NOTE: The density of cell suspension is to obtain a density of 10,000 cells per well in the agarose-coated 96-well plate.

4.7.2. Centrifuge the plate at 340 *x g* for 10 minutes and incubate at 5% $CO_2$ at 37°C for 5-9 days (**Figure 1D**).

NOTE: Change medium every other day after plating with gentle removal of 50% of cDMEM and replacement.

NOTE: HFF/MRC-5 spheroids can be used for the HEP-MES assembloid model.

## 5. HepG2-WT and HFF/MRC-5 Assembloid Formation

NOTE: Refer to Sections 3 and 4 for formation of HepG2 (**Figure 2A)** and HFF/MRC-5 spheroids (**Figure 2B**).

5.1. Individually collect HFF/MRC-5 spheroids using a pipette from the 96-well plate and transfer them to a 15 mL sterile conical centrifuge tube. Allow the spheroids to settle and gently rinse with warm cDMEM.

NOTE: This rinsing process should be done very gently and carefully.

5.2. Transfer a single HFF/MRC-5 spheroid to a well containing a HepG2-WT spheroid and add MG/CG between a 1:1 and 1:5 dilution and incubate at 37°C at 5% $CO_2$ for 3 hours.

5.3. Add 75 uL of cDMEM to each well and incubate at 37°C at 5% $CO_2$ for 2-3 days (**Figure 2C**).

NOTE: Change medium every other day after plating with gentle removal of 50% of cDMEM and replacement. Assembloids will still form without media changes for up to 3-4 days.

NOTE: Assembloid formation can occur without the use of matrix.

## 6. HepG2-WT Spheroid Droplet Formation

NOTE: Refer to Section 3 for formation of HepG2 spheroids (**Figure 3A**).

NOTE: Two different materials can be used for suspending the HepG2-WT spheroids in droplets. The two methods are provided below.

6.1. Matrigel (MG) droplets

6.1.1. Mix 1 mL of ice-cold diluted MG and control growth medium at a 1:1 dilution. Mix the spheroid/MG suspension and distribute it evenly inside the MG solution.

6.1.2. Collect the HepG2-WT spheroids in a 15 mL sterile conical centrifuge tube on ice and allow the spheroids to settle. Aspirate the medium and keep it on ice.

6.1.3. Using a 200 µL pipette, collect a 15 µL volume of one spheroid in MG solution and seed onto a 60 mm petri dish (**Figure 3B**).

6.2. Collagen (CG) Droplets

NOTE: All collagen preparation should be done on ice.

6.2.1. In a microcentrifuge tube, add 358.8 µL of de-ionized water, 100 µL of 10X PBS, 12.1 µL of 1 N NaOH, and 529.1 µL of stock rat tail CG for a total volume of 1 mL. Mix the spheroid/CG suspension and distribute it evenly inside the CG solution.

NOTE: Stock rat tail CG should always be added at the end.

6.2.2. Collect the HepG2-WT spheroids in a 15 mL sterile conical centrifuge tube on ice and allow the spheroids to settle. Aspirate the medium and keep it on ice (**Figure 3B**).

6.2.3. Using a 200 µL pipette, collect a 15 µL volume of one spheroid in CG solution and seed onto a 60 mm petri dish.

NOTE: If more than one spheroid is seeded per droplet, it is removed and reseeded properly.

NOTE: Spheroid/CG solutions are pipetted slowly onto the 60 mm petri dish to avoid air bubbles.

6.3 Incubate the droplet at 37°C for 60 minutes before the addition of the growth medium.

6.4 Slowly add 5 mL of desired growth medium to the petri dish and incubate in at 37°C and 5% $CO_2$ with medium changes every three days (**Figure 3C**).

NOTE: HFF/MRC-5 conditioned-media was used in the droplet formation assay.

## 7. Preparation of HFF/MRC-5 Conditioned Media (M-CM)

7.1. Seed HFF/MRC-5 into a T-75 tissue culture-treated flask at a seeding density of 5,000 cells/$cm^2$ and incubate the flask for 72 hours in 15 mL of cDMEM.

NOTE: Flask should be checked daily during this period to ensure the maintenance of cell health.

7.2. After the 72-hour incubation, collect the fibroblast-conditioned growth medium in a 15 mL sterile conical centrifuge tube. Centrifuge the fibroblast-conditioned growth medium at 290 *x g* for 5 minutes and filter using a 0.2 µm filter (**Figure 4A**).

7.3. Dilute the fibroblast-conditioned growth medium with complete growth medium at a 1:1 to 1:7 dilution ratio and add to the desired experiment (**Figure 4B**).

## 8. HepG2-WT and HFF/MRC-5 Mixed Spheroid Formation

NOTE: Refer to Sections 3 and 4 for formation of HepG2 (**Figure 5A)** and HFF/MRC-5 spheroids (**Figure 5B**).

8.1. Transfer HepG2-WT and HFF/MRC-5 cell suspension to a 15 mL sterile conical centrifuge tube at a 1:1 ratio to obtain a final concentration of 2.0 x $10^5$ cells/mL. Mix the cell suspension very well and transfer 100 µL of cell suspension per well to the agarose-coated 96-well plate.

NOTE: The density of cell suspension is to obtain a density of 20,000 cells per well in the agarose-coated 96-well plate.

8.2. Centrifuge the plate at 340 *x g* for 10 minutes and incubate at 5% $CO_2$ at 37°C for 1-2 days (**Figure 5C**).

NOTE: Change medium every other day after plating with gentle removal of 50% of cDMEM and replacement.

## REPRESENTATIVE RESULTS:

Currently, there is increased interest in synthetic tissues for various biomedical applications, including modeling disease, discovering drugs, and tissue engineering (**Figure 6**). In this field, hPSC-derived organoids or spheroids, and cells can be converted into more synthetic, complex, and larger tissues. To accomplish this, principles of morphogenesis, tools like microfabrication, and biomatrices can be applied to cells and spheroids to engineer these synthetic tissues more precisely (**Figure 6**). We present several methods here with this theme in mind.

### *Effects of clustering on spheroid formation*

The methods developed here were contingent upon successful 3D spheroid formation. Spheroid formation is considered successful if cells fuse to form a full spheroid within five to nine days. An early indication of successful spheroid formation is clustering of the cells in the center of the well after centrifugation of the cultivation plate. Despite the significance of clustering, spheroid formation did occur, but less frequently, when cells were initially scattered rather than clustered, therefore demonstrating that successful spheroid formation could still occur. Spheroid formation is considered unsuccessful if cells do not spread and fuse together within nine days after plating.

Spheroids were cultured at two different sizes to perform this experiment; small spheroids (S) were plated at a concentration of 1,500 cells per well and large spheroids

(L) were plated at a concentration of 3,000 cells per well. Hepatic spheroids compacted and fully cultured by day five, irrespective of the spheroid size. The cell density per well did not impact the rate at which the spheroid formed and had a significant difference in spheroid size (**Figure 7**). In this case, it is important to observe an increase in opacity which demonstrates thickening of the initial disc-shaped tissue, which is more translucent, to a spheroid configuration, which has increased opacity. Unlike hepatic spheroids, mesodermal-derived spheroids compacted within 24 hours irrespective of cell seeding density as well. Notably, HFF/MRC-5 cells compact much tighter than HepG2-WT cells, likely resulting in cell density having little impact on spheroid size.

***Factors that affect hepatic and mesenchymal (mesodermal-derived) assembloid formation***

Hepatic and mesodermal-derived spheroids of varying sizes were cultured to determine the effect of size on the compaction time of spheroid formation. Hepatic and mesodermal-derived spheroids were co-cultured in Matrigel (MG) or Collagen Gel (CG) at a 1:5 dilution with complete growth medium or fibroblast-conditioned medium, to determine if matrix and conditioned medium influences assembloid formation. Both cell types were dye-labeled prior to spheroid formation to demonstrate the interaction between spheroids. It was observed that assembloid formation occurs irrespective of matrix and medium (**Figure 8**). We studied the effects of CG, effects of MG, and effects of conditioned medium (MRC-5 conditioned medium or MCM-5). We observed assembloid formation in all cases, although the morphological details varied slightly (**Figure 8**). Details regarding these images will be re-used in later figures. To determine the effects of inter-spheroid distance on assembloid formation, distance was measured together with success of assembloid formation. It was observed that the compaction time of an assembloid is directly proportional to the initial distance of the hepatic and mesodermal-derived spheroids (**Table 1**).

***Building more complex assembloids with arm-like structures***

Methods were also developed to build assembloids that have branching cords (**Figure 9A**). To accomplish this experimentally, hepatic spheroids are mixed with biomatrix (MG), in 384-well plate, and surrounded by single fibroblasts at high density. These fibroblasts cluster and provide guides to which hepatic cells migrate towards and thicken, forming thick cords over time. Hepatic spheroids were cultivated in the MG droplet system containing a high density of MRC-5 cells (300,000 cells) in 384-wells and demonstrated small clusters of MRC-5 cells that formed in the MG (**Figure 9B, days 3-4**). Next, the liver spheroids formed thick migrating strands protruding out to the fibroblast clusters forming thick strands containing both cell lines (**Figure 9B, days 9-12**). This approach led to longer arms or cords, likely containing a mix of hepatic and fibroblast cells. Another approach involved building bridges or small interconnections (arms) between spheroids. To build small armed structures, a larger HEP spheroid can be co-cultured in 384-well plate with a smaller mixed spheroid (**Figure 9C**). This leads to small, knob-like arms. Overall, we present two approaches for forming additional arms to spheroids.

***Spot-welding (fused edges) of complex assembloids***

Methods were used to build assembloid with fused edges. Hepatic, and mesodermal-

457 derived spheroids are placed in a stiff environment of CG (2 mg/mL) **(Figure 9D)**.
458 Furthermore, in this stiff environment, rather than cupping, we observe spheroids fuse at
459 the edges to form assembloids with evidence of short arms, or spot-welding (**Figure 9E**).
460 We see similar data with MRC5 Fibroblasts in CG (**Figure 9F**).
461
462 ***Infiltrating and layering of complex assembloids***
463 During liver organogenesis, in the developing liver diverticulum, HEP cells are
464 surrounded by mesenchyme, and ultimately, they migrate or infiltrate into the
465 mesenchyme (**Figure 9G**). In M-CM, and CG conditions, the addition of MES and HEP
466 spheroids results in a different type of fusion in which we observe an infiltrative pattern
467 (**Figure 9H**). Further, we can obtain a layering pattern by placing single MES (human
468 mesenchymal stem cells (hMSC)) in MG at high density and allowing them to migrate
469 towards a HEP spheroid and layer on the surface without infiltration, as shown with dye
470 labeling of the hMSC (**Figure 9I**). We note that this is a different phenotype than when
471 we employed HFF. This latter arrangement is observed in the liver diverticulum stage and
472 many other endoderm-derived tissues. Here we present two approaches that are relevant
473 for modeling of the developing liver diverticulum and for creating aspects of synthetic
474 tissues.
475
476 ***Fused hepatic and mesenchymal (mesodermal-derived) assembloid formation***
477 The fusion of two spheroids to form assembloids are critical for modeling the liver
478 bud. This is because when two spheroids fuse, the cells likely migrate on top or between
479 other cells, which we term interstitial migration. Interstitial migration occurs in the liver
480 bud, when early migrating hepatoblasts migrate through mesenchyme, potentially on top
481 of other cells. Therefore, fusion of two spheroids is a model of interstitial migration which
482 occurs during liver organogenesis. Methods were developed to build assembloids that
483 fuse completely with separate layers (**Figure 10A**). HEP and MES (MRC5 fibroblasts)
484 spheroids in MG form a fused assembloid by day 9 (**Figure 10B**). Dye-labeling analysis
485 demonstrated that MES tissue remained inside, while the HEP tissue remained outside
486 (**Figure 10C**). Importantly, the final spheroid is approximately the same size as the
487 original spheroids. This suggests that the cells are packed at high density. Notably, the
488 same phenomena occur in the absence of MG in 384-well plates, when multiple MES
489 spheroids are placed with a single HEP spheroid (**Figure 10D**). HEP-MES assembloids,
490 in the absence of matrix, also form under low serum (2% FBS) and extremely low serum
491 (0.2% FBS) conditions (**Figure 10E**). We then determined that large distances
492 (approximately 3 diameters of the spheroid), assembloids did not form (**Figure 10F**). To
493 determine how spheroid composition determines spheroid fusion, we demonstrated that
494 mixed spheroids (containing MES and HEP cells) can fuse with MES spheroids by day 5,
495 accompanied by an increased packing density, as expected (**Figure 10G**).
496
497 ***Partially fused or cupping in complex assembloid formation***
498 Successful assembloid formation in MG demonstrates several phenotypes,
499 including the observation that the HEP spheroid undergoes “cupping” of the MES
500 spheroid to form a partially fused assembloid (**Figure 10H**). This also establishes a visual
501 model of interstitial migration, and points toward the current mechanism of fused
502 assembloid formation. Time series studies of HEP and MES spheroids demonstrate with

in CG, fusion occurs via a cup-like mechanism (**Figure 10I**). This is further demonstrated using dye-labeling (**Figure 10J**). Finally, the same phenomena is clearly illustrated when multiple HEP spheroids are used with a large, single MES spheroid (**Figure 10K**). The data suggests that cupping without fusion can occur in MG or in cases where the MES spheroid is much larger than the HEP spheroids.

***Induced hepatic branching and linear migration via mesenchymal (mesodermal-derived) conditioned growth medium***

Collective migration is a key morphogenetic process during liver organogenesis. Here we describe tools for inducing collective migration *in vitro*. Successful droplet formation of HEP spheroids and utilization of M-CM (MES-conditioned media) demonstrate outgrowth branching from the HEP spheroids (**Figure 11A-B**). HEP spheroids cultivated in the MG droplet system demonstrated that M-CM induces collective migration, and the data demonstrates a concentration-dependent effect (**Figure 11B, right**). Cellular strands protruding from the hepatic spheroid are present with small branching, thick strands, and multiple levels of branching (**Figure 11B, left**). On day 11, the protrusions were increased with inter-connections and sheet formation (**Figure 11B, right**). M-CM is potent, as a 1:7 dilution or M-CM present for one day still leads to migration (**Figure 11B, right**). It was hypothesized that the M-CM induced cell migration via TGFβ signaling pathway. A83-01, a TGFβ pathway inhibitor, was incorporated into the M-CM at varying concentrations, and migration was significantly inhibited in a dose-dependent manner (**Figure 11C**). To determine the effects of extracellular matrix on collective migration, HEP spheroids cultivated in the CG droplet system demonstrate that M-CM induces cell migration. However, the protrusions were thin linear strands and less branching by day 7 compared to the migration observed in MG (**Figure 11D**). We also tested fibrin hydrogels, and we observed thin, hair-like, narrow, radial protrusions of both HEP and MES cells (**Figure 11E**).

***Inducing hepatic co-migration via MES conditioned medium***

Mixed spheroids (HEP-MES spheroids) were also employed for collective migration, as a model of co-migration which occurs during early liver organogenesis (**Figure 11F**). These mixed spheroids in MG result in migration, and when TGFβ1 growth factor was added, it resulted in significantly increased collective migration (**Figure 11G**). Thus, co-migration can also be modeled with mixed spheroids.

**FIGURE AND TABLE LEGENDS:**

**Figure 1. Schematic of spheroid formation assay. (A)** Coating of a 96-well plate with 1% agarose solution. The agarose solution is warmed in the microwave until it is in the liquid phase and cooled prior to use. 55-65 µL of agarose solution is transferred to each well and the plate is cooled in the fridge for 20-30 minutes. **(B)** Passaging of cell culture at 80% confluency. **(C)** Dye labeling of cell suspension. 5 µL of cell-labeling solution is added per mL of cell suspension and incubated for 20 minutes. The cell suspension is centrifuged at 450 *x g* for 5 minutes and washed with warm cDMEM three times prior to plating the cells. The cell suspension is diluted to the desired cell density per well. **(D)** Plating of cell suspension for spheroid formation. 100 µL of cell suspension is added to each well and centrifuged at 340 *x g* for 10 minutes. Mesodermal-derived spheroids are

incubated for 1-3 days until spheroid formation is complete. Hepatic spheroids are incubated for 5-9 days until spheroid formation is complete.

**Figure 2. Schematic of assembloid formation assay with hepatic and mesodermal-derived spheroids. (A)** Hepatic spheroid formation. HepG2-WT cells are dye-labeled with a cell-labeling solution and plated for spheroid formation. **(B)** Mesodermal-derived spheroid formation. HFF/MRC-5 cells are dye-labeling solution and plated for spheroid formation. **(C)** Transferring mesodermal-derived spheroid to hepatic spheroid for assembloid formation. Matrix (Matrigel or Collagen) is added to the well at a 1:1-1:5 dilution range and incubated for 3 hours. 75 µL of cDMEM is added to the well and is incubated for 2-3 days until assembloid formation is complete.

**Figure 3. Schematic of Droplet Formation Assay. (A)** Hepatic spheroid formation. HepG2-WT cells are dye-labeled with a cell-labeling solution and plated for spheroid formation. **(B)** Hepatic spheroids are collected and gently rinsed with cDMEM. The spheroids are suspended in a matrix (Matrigel or Collagen). **(C)** Hepatic spheroids are seeded onto a 60mm petri dish and incubated for 60 minutes. 5 mL of fibroblast-conditioned media is added to the petri dish and incubated with media changes every three days.

**Figure 4. Schematic of Preparation of Fibroblast-Conditioned Media. (A)** Cells are seeded at 5,000 cells/cm2 in a T-75 and incubated for 72 hours. The media is collected and sterilized prior to use. **(B)** Sterilized conditioned media is diluted with cDMEM at a 1:1-1:7 dilution and added to a hepatic spheroid in a pre-existing well. The spheroid is incubated, and the media is changed every three days.

**Figure 5. Schematic of Hepatic and Mesodermal-derived Mixed Spheroid Formation Assay. (A)** Preparation of Hepatic cell suspension. HepG2-WT cells are harvested and dye-labeled with a cell-labeling solution. **(B)** Preparation of Mesodermal-derived cell suspension. HFF/MRC-5 cells are harvested and dye-labeled with a cell-labeling solution. **(C)** Mixed Spheroid Formation. HepG2-WT and HFF/MRC-5 cells are mixed at a 1:1 ratio at a final concentration of 2.0 x 105 cells/mL and plated for spheroid formation. The plate is incubated for 1-2 days until mixed spheroid formation is complete.

**Figure 6. Overview.** Based in the science of morphogenesis (top), stem cells will be implemented to build assembloids. The toolbox (middle), through the use of cells, tools, and biomatrix, and together with aspects of morphogenesis, can together be used to generate new synthetic tissues and assembloids.

**Figure 7. Compaction time of varying HepG2-WT spheroid size.** Progression of hepatic spheroid formation of varying sizes over a five-day period. Spheroids were plated at 1,500 cells per well (small) and 3,000 cells per well (large) and observed for five days. Spheroid formation was observed to occur under both conditions within five days.

**Figure 8. The effect of media and matrix on assembloid formation.** Hepatic spheroids and mesodermal-derived spheroids were transferred to an agarose-coated well. The cells

were dye-labeled prior to spheroid formation to demonstrate the interaction between spheroids. The spheroids were suspended in a 1:5 solution of the matrix (Matrigel or Collagen) and cDMEM or fibroblast-conditioned media (M-CM) and observed for four days (MRC-5 is orange, HepG2-WT is green). It was observed that assembloid formation occurred under the four conditions.

**Figure 9. Engineering assembloids arms, junctions, and layers. (A)** Building of large and small arms onto hepatic spheroids. **(B)** Phase-contrast microscopy images of hepatic spheroids containing growth factor-free (GFR) cultured in the MG droplet system, bearing high density (30,000 cells) of MRC-5 cells were cultured for 12 days. Top row, left to right: days 3, 4, 9, and 12. Day 3: MRC-5 cells initially after seeding (arrow). Bar = 1,000 µm. Day 4: MRC-5 cells spreading and interconnecting (arrows). Bar = 1,000 µm. Day 9: Thick hepatic cord (arrows). Bar = 400 µm. Day 12: multiple, thick hepatic cords. Bar = 400 µm. Bottom row, left to right: each image in a separate experimental replicate on day 12 demonstrating thick hepatic cord formation (arrows). Bar = 400 µm. **(C)** Fluorescent images of hepatic spheroid (figure 1) co-cultured with a HEP-MES mixed spheroid (figure 5) on days 0 and 5. It was observed on day five, that the HEP-MES mixed spheroid fused with the edge of the hepatic spheroid to form a bridge. **(D)** Fused HEP-MES assembloids, which are the same size as original spheroids, with the edges of the two spheroids fused to create an assembloid. These spheroids create a higher packing density once combined into an assembloid. **(E)** Phase-contrast images of hepatic and mesodermal-derived spheroids in the CG droplet system cultivated in M-CM. Collagen provides stiff conditions during assembloid formation. By day 4, it was observed that HEP-MES cultured in M-CM fuses the edges of the spheroids and does not form cupping. **(F)** In the CG droplet system, the HEP-MES assembloid edges are fused together. The left image is a phase-contrasted image, and the right is a fluorescent image to show the fusion of hepatic and mesodermal-derived spheroids. The hepatic spheroid is dye-labeled green, and the MRC-5 spheroid is dye-labeled orange in the figure. **(G)** The left image shows HEP-MES infiltrating assembloid and the right image demonstrates a surface-MES layered assembloid. **(H)** Infiltration of HEP-MES spheroids in collagen matrix with MES-conditioned media (M-CM). Left- phase-contrast image of assembloid. Right-fluorescent image showing infiltration of HEP and MES spheroids forming assembloid. **(I)** Phase (left), double fluorescent (red/green) images (right) of days 4, 5, and 6 LD models, bearing a HepG2-GFP spheroid (green) and MSC (red) in MG. The right columns on the right are replicates 1 and 2 with double fluorescent images on days 4, 5, and 6. This is an example of layering without infiltration of the spheroids to form an assembloid. Data was replicated to prove the outcome described. Bar = 500 µm. Adopted with permission of publisher from Ogechi, Parashurama et al., 2021 (Ogechi et al., 2021).

**Figure 10. Partially and completely fused HEP-MES assembloids. (A)** Fused HEP-MES assembloids, which are the same size as the original spheroids, thus increasing packing density. **(B)** Phase-contrast images of HEP and MES spheroids cultivated in MG droplet system. It was observed that by day 11, assembloid formation had occurred which typically occurs in 2-5 days. **(C)** Fluorescent images of HEP-MES assembloid on day 13. It was observed that assembloid formation had occurred with separate layers, MES (red) surrounded by the HEP (green). **(D)** Phase-contrast images of hepatic spheroid co-

cultured with multiple mesodermal-derived spheroids. By day 5, it was observed that the HEP-MES assembloid did not increase in volume. **(E)** HEP-MES assembloids fuse under low serum. HepG2-WT spheroids and HFF/MRC-5 cells were plated (figure 1) and suspended in low serum FBS (2% and 0.2%). Top- 2% FBS to fuse HEP-MES assembloid. Bottom- 0.2% FBS to fuse HEP-MES assembloid. It was observed that HEP-MES assembloid formation occurred over a period of two days. **(F)** Phase-contrast images of hepatic and mesodermal-derived spheroids in the CG droplet system cultivated in M-CM. When the spheroids are placed at large distances in the CG droplet system, assembloid formation does not occur. **(G)** Fluorescent images of hepatic spheroid (**Figure 1**) co-cultured with a HEP-MES mixed spheroid (**Figure 5**) on days 0 and 5. It was observed on day five, that the HEP-MES mixed spheroid fused with the edge of the hepatic spheroid to form a bridge. **(H)** Cupping or partially fused HEP-MES assembloid. The packing density of the spheroid is increased and has separate layers. **(I)** HEP tissue (H) forms cup structure around MES tissue cultivated in the CG droplet system before fusing. By day 4, we see assembloid formation occur in a cup-like mechanism. **(J)** HEP-MES cupping prior to fusion in Matrigel. The left images are phase contrast, and the right-side images are fluorescent. Top- day two of formation. Bottom- day four of partial fusion is noticeable. **(K)** HEP-MES assembloids with multiple hepatic spheroids combine through the cupping mechanism. Day 5 hepatic spheroids form a cup around mesodermal tissue. Adopted with permission of publisher from Ogechi, Parashurama et al., 2021 (Ogechi et al., 2021).

**Figure 11. Methods for modulating collective migration from spheroids. (A)** Branching and linear migration in hepatic spheroids in the presence of M-CM. **(B)** Phase-contrast images of day 7 and day 11 hepatic spheroids in the Matrigel (MG) droplet system cultivated in varying dilutions of M-CM. By day seven, the hepatic spheroid demonstrated 3D collective cell migration. The area was measured for varying dilution ratios. Analysis of Matrigel droplet system with M-CM. A plot of fold change in the area across different M-CM dilutions (1:1, 1:7, M-CM 1 day, and M-CM). Comparison of M-CM with 1:1 condition ($P = 0.15$, $n = 3$ for both conditions), M-CM with 1:7 condition ($P = 0.0056$, $n = 3$ for both conditions), and M-CM with M-CM 1-day-only condition ($P = 0.019$, $n = 3$ for both conditions). **(C)** Phase-contrast images on day 7 of Hepatic spheroids in MG droplet system cultivated in M-CM alone, M-CM with A83-01 (10 nM), and A83-01 (20 nM). Bar graph analysis comparing day 7 M-CM and M-CM + A83-01 (20 nM) ($P = 0.047$, $n = 3$). Plotted means ± SD. Significance is defined as $P \leq 0.05$. **(D)** Phase-contrast images on days 4 and 7 of the hepatic spheroid in the collagen (CG) droplet system cultivated in M-CM medium. Arrows specify thin filopodia-like extensions into the collagen. Bar graph analysis of Hepatic spheroids in collagen (CG) in cDMEM (control) and M-CM conditions comparing protrusion length ($P = 0.012$, $n = 3$). **(E)** Fluorescent images of day 5 HEP-MES mixed spheroid in Fibrin gels cultivated in M-CM. **(F)** Star-shaped migration of HEP-MES mixed spheroids. **(G)** Fluorescent images of day 4 of HEPG2-GFP (HepG2 cells expressing green fluorescent protein) and MES mixed spheroids in the MG droplet system after treatment with TGFβ1 (20 ng/ml). From left to right: HepG2 (green) cells and combined HepG2 (red) and MRC-5 (yellow) images. Replicates 2 (above) and 1 (below) are shown. Arrows show HepG2 and MRC-5 migration. Bar graph comparing the area of fibroblast migration in the negative control

(HepG2-GFP/MRC-5) and (HepG2-GFP/MRC-5 + TGFβ1, 20 ng/ml), P = 0.012, n = 3. Plotted means ± SD. Significance is defined as P ≤ 0.05. ∗ is used to denote the significance of experimental data. Adopted with permission of publisher from Ogechi, Parashurama et al., 2021 (Ogechi et al., 2021).

**Table 1. The effect of distance on assembloid formation.** Hepatic spheroids and mesodermal-derived spheroids were transferred to an agarose-coated well. The cells were dye-labeled prior to spheroid formation to demonstrate the interaction between spheroids. The spheroids were suspended in a 1:5 solution of the matrix (Matrigel or Collagen) and cDMEM or fibroblast-conditioned media (M-CM). The initial distance between the spheroids was measured using ImageJ and the corresponding compaction time of the assembloid formation was observed. The compaction time of assembloid formation is directly proportional to the initial distance between the spheroids, irrespective of the matrix or media.

## DISCUSSION:

In this protocol, several methods are presented for cultivating simple and complex assembloids, and methods for inducing 3D collective cell migration in early liver organogenesis. We have presented several protocols many of which have critical steps. Spheroid formation is a critical step in the process in all these methods. Spheroid formation can be accomplished using microwells (96- or 384-wells) with either non-adherent or agarose-coated plates. Considerable expertise is needed to handle organoids regarding formation of spheroids (or organoids), transferring between wells, addition of biomatrices upon spheroids, and addition of multiple spheroids per well. Formation of the spheroids requires critical attention to repeatable cell counting and seeding, agarose coating (or non-adherent), regular medium changes, dye-labeling methods, and gentle handling of spheroids and plates together with microscopy. We also note that dye-labeling should be experimentally determined in terms of cell number and type, and amount of labeling time.

For example, preparation of agarose solution must be stringent in terms of maintaining appropriate concentrations and seeding wells with appropriate volumes, such that a meniscus (curvature develops) and enables collection of cells in the center. We recommend careful attention to agarose concentration, volumes, and solidification of gel. Determining correct micropipette tip size and transferring techniques is critical for proper handling of spheroids. Glass wells can be used for improved visualization. As we have noted in the paper, spheroids can first appear as translucent discs that become more opaque over time, which can be used to monitor spheroid formation, and several factors affect this time. Finally, assembloid formation requires careful transfer of spheroids, and they need to be placed within a couple of spheroid diameters or less to effectively observe changes.

Here, using cell lines, a toolbox of methods to develop complex assembloids and migrating spheroids have been created. It is important to note that cell lines were employed. While this enabled focus upon methods, using primary cells or hPSC-derived cells would be advantageous with the use of human personalized tissues. We can

validate that our assembloid techniques work with hPSC-derived HEP cells. A significant limitation of these systems is the matrix. Matrigel, a mouse tumor extracellular matrix protein mixture, is primarily used as the matrix in these cultivation models. However, it is a major limitation due to its tumor-derived origin and high cost. Furthermore, the droplet formation system can only last 2 weeks before significantly degrade, and thus alternative gels could be implemented such as collagen mixtures or sodium alginate. Furthermore, the current systems can only grow to on the order of dimensions of the spheroids, but not beyond. Thus, determining and addressing limitations to growth is critical.

There is a lack of methods to specifically study early events in early liver organogenesis, and more generally, methods to generate synthetic tissues. The methods developed here address this gap. With further study and characterization, he assembloids and tissues we generate can be used to build larger tissues that can be used for improved modeling of solid tissues and organs. This is not currently possible using current techniques.

These methods provide a toolbox that can be used to further build assembloids and assemble larger, more complex tissues for better *ex vivo* organ modeling, and potentially for *in vivo* therapeutic approaches, in addition to modeling structures during organogenesis (liver bud) and being employed for biopharma applications.

The protocols we develop here enable models of different modes of liver cell migration such as, co-migration, interstitial migration, and branching morphogenesis, as well as assembloids that, together, can be used to build more complex tissues for various biomedical and biopharma applications.

**ACKNOWLEDGMENTS:**

NP was supported by the UB CBE startup funds, a Mark Diamond Fellowship, the New York State Stem Cell Science C024316, the UB the Stem cells in regenerative medicine (ScIRM) center, the University at Buffalo Center for Cell, Gene, Tissue Engineering (CGTE).

**DISCLOSURES:**

NP is the founder of Khufu Therapeutics, an organoid engineering company that develops treatments for acute and chronic liver disease.

**REFERENCES:**

Binamé, F., P. Lassus and U. Hibner (2008). "Transforming growth factor beta controls the directional migration of hepatocyte cohorts by modulating their adhesion to fibronectin." Mol Biol Cell **19**(3): 945-956.

Bort, R., M. Signore, K. Tremblay, J. P. Martinez Barbera and K. S. Zaret (2006). "Hex homeobox gene controls the transition of the endoderm to a pseudostratified, cell emergent epithelium for liver bud development." Dev Biol **290**(1): 44-56.

Chen, J. S., L. L. Liang, H. X. Xu, F. Chen, S. L. Shen, W. Chen, L. Z. Chen, Q. Su, L. J. Zhang, J. Bi, W. T. Zeng, W. Li, N. Ma and X. H. Huang (2017). "miR-338-3p inhibits epithelial-mesenchymal transition and metastasis in hepatocellular carcinoma cells." Oncotarget **8**(42): 71418-71429.

Fitamant, J., F. Kottakis, S. Benhamouche, H. S. Tian, N. Chuvin, C. A. Parachoniak, J. M. Nagle, R. M. Perera, M. Lapouge, V. Deshpande, A. X. Zhu, A. Lai, B. Min, Y. Hoshida, J. Avruch, D. Sia, G. Camprecios, A. I. McClatchey, J. M. Llovet, D. Morrissey, L. Raj and N. Bardeesy (2015). "YAP Inhibition Restores Hepatocyte Differentiation in Advanced HCC, Leading to Tumor Regression." Cell Rep **10**(10): 1692-1707.

Fransvea, E., U. Angelotti, S. Antonaci and G. Giannelli (2008). "Blocking transforming growth factor-beta up-regulates E-cadherin and reduces migration and invasion of hepatocellular carcinoma cells." Hepatology **47**(5): 1557-1566.

Gualdi, R., P. Bossard, M. Zheng, Y. Hamada, J. R. Coleman and K. S. Zaret (1996). "Hepatic specification of the gut endoderm in vitro: cell signaling and transcriptional control." Genes Dev **10**(13): 1670-1682.

Gupta, S., P. Rajvanshi, R. Sokhi, S. Slehria, A. Yam, A. Kerr and P. M. Novikoff (1999). "Entry and integration of transplanted hepatocytes in rat liver plates occur by disruption of hepatic sinusoidal endothelium." Hepatology **29**(2): 509-519.

Koenig, S., C. Stoesser, P. Krause, H. Becker and P. M. Markus (2005). "Liver Repopulation after Hepatocellular Transplantation: Integration and Interaction of Transplanted Hepatocytes in the Host." Cell Transplantation **14**(1): 31-40.

Matchett KP, W.-K., Portman jr, Kapourani CA, Feroq F, May S, Mackey JBG, Brice M, Zajdel E, Beltran M, Sutherland EF, Wilson GC, Wallace SJ, Kitto L, Youngeer NT, Dobie R, Oniscu GC, Wigmore SJ, Ramchandran P, Vallejos CA, Carragher NO, Simpson KJ, Kendall TJ, Acute Liver Failure Study Group; Rule JA, Lee WM, Hoare M, Weston CJ, Marioni JC, Teichmann ST, Bird TG, Carlin LM, Henderson NC. (2023). "Multimodal decoding of human liver regeneration." bioRxiv Pre-print Server.

Matsumoto, K., H. Yoshitomi, J. Rossant and K. S. Zaret (2001). "Liver organogenesis promoted by endothelial cells prior to vascular function." Science **294**(5542): 559-563.

Ng, L., R. Tung-Ping Poon, S. Yau, A. Chow, C. Lam, H. S. Li, T. Chung-Cheung Yau, W. L. Law and R. Pang (2013). "Suppression of actopaxin impairs hepatocellular carcinoma metastasis through modulation of cell migration and invasion." Hepatology **58**(2): 667-679.

Ogoke, O., J. Oluwole and N. Parashurama (2017). "Bioengineering considerations in liver regenerative medicine." J Biol Eng **11**: 46.

Ogoke O., G. D., Thompson S., Chiang A., Ngyuen TH., Berke D., Ott C., Kalinousky A., Shamul C., Chen P., Ross S., Chen Z., Srivastava P., Mahajan S., Zhao R., Gunawan R., Parashurama N. (2022). "Dynamic changes in the niche and transcription trigger early murine and human pluripotent stem cell-derived liver organogenesis." BioRxiv (Pre-print server) **10.1101/2022.07.24.501313**.

Petkov, P. M., K. Kim, J. Sandhu, D. A. Shafritz and M. D. Dabeva (2000). "Identification of Differentially Expressed Genes in Epithelial Stem/Progenitor Cells of Fetal Rat Liver." Genomics **68**(2): 197-209.

Rajvanshi, P., A. Kerr, K. K. Bhargava, R. D. Burk and S. Gupta (1996). "Studies of liver repopulation using the dipeptidyl peptidase IV-deficient rat and other rodent recipients: cell size and structure relationships regulate capacity for increased transplanted hepatocyte mass in the liver lobule." Hepatology **23**(3): 482-496.

Rossi, J. M., N. R. Dunn, B. L. Hogan and K. S. Zaret (2001). "Distinct mesodermal signals, including BMPs from the septum transversum mesenchyme, are required in combination for hepatogenesis from the endoderm." Genes Dev **15**(15): 1998-2009.

Sosa-Pineda, B., J. T. Wigle and G. Oliver (2000). "Hepatocyte migration during liver development requires Prox1." Nat Genet **25**(3): 254-255.

Suzuki, A., S. Sekiya, D. Büscher, J. C. Izpisúa Belmonte and H. Taniguchi (2008). "Tbx3 controls the fate of hepatic progenitor cells in liver development by suppressing p19ARF expression." Development **135**(9): 1589-1595.

Xue, T. C., N. L. Ge, L. Zhang, J. F. Cui, R. X. Chen, Y. You, S. L. Ye and Z. G. Ren (2014). "Goosecoid promotes the metastasis of hepatocellular carcinoma by modulating the epithelial-mesenchymal transition." PLoS One **9**(10): e109695.

Yang, C., Y. Xu, F. Cheng, Y. Hu, S. Yang, J. Rao and X. Wang (2017). "miR-1301 inhibits hepatocellular carcinoma cell migration, invasion, and angiogenesis by decreasing Wnt/beta-catenin signaling through targeting BCL9." Cell Death Dis **8**(8): e2999.

Yang, M. H., C. L. Chen, G. Y. Chau, S. H. Chiou, C. W. Su, T. Y. Chou, W. L. Peng and J. C. Wu (2009). "Comprehensive analysis of the independent effect of twist and snail in promoting metastasis of hepatocellular carcinoma." Hepatology **50**(5): 1464-1474.

Zeng, Y. B., X. H. Liang, G. X. Zhang, N. Jiang, T. Zhang, J. Y. Huang, L. Zhang and X. C. Zeng (2016). "miRNA-135a promotes hepatocellular carcinoma cell migration and invasion by targeting forkhead box O1." Cancer Cell Int **16**: 63.

Zhao, Y., W. Jian, W. Gao, Y.-X. Zheng, Y.-K. Wang, Z.-Q. Zhou, H. Zhang and C.-J. Wang (2013). "RNAi silencing of c-Myc inhibits cell migration, invasion, and proliferation in HepG2 human hepatocellular carcinoma cell line: c-Myc silencing in hepatocellular carcinoma cell." Cancer Cell International **13**(1): 23.

A

Heat 1% agarose solution in microwave and allow to cool prior to use

Transfer 55-65 µL of agarose solution per well

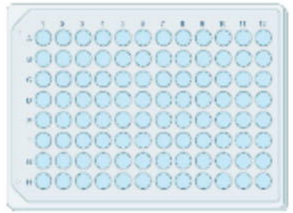

Cool the plate for 20-30 mins at 4°C and bring to room temperature

B

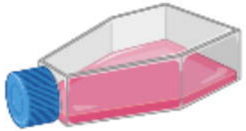

Cell culture has reached 80% confluency

Passage cells using Tryspin-EDTA

Suspend cells at a density of 1 x $10^6$ cells/mL of serum-free medium and add 5 uL of cell-labeling solution

C

Add 5 uL of cell-labeling solution per mL and incubate for 20 mins

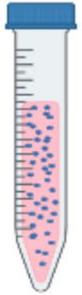

Centrifuge at 450 *x g* for 5 mins and wash cells with cDMEM. Repeat this wash process two more times.

D


Add 100 µl of cell suspension to per agarose-coated well and centrifuge at 340 *x g* for 10 mins

mesodermal-derived spheroid


Incubate for 1-3 days until spheroid formation is complete (mesodermal-derived spheroid)

hepatic spheroid


Incubate for 5-9 days until spheroid formation is complete (hepatic spheroid)

A

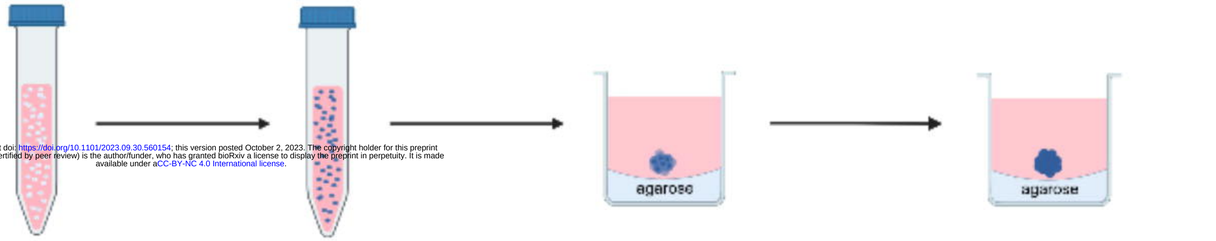


Passage HepG2-WT cell culture. Suspend cells at a density of 1 x $10^6$ cells/mL

Dye-label the cells and suspend at a density of 5 x $10^4$ cells/mL

Add 100 µl of cell suspension to per well and centrifuge 340 *x g* for 10 mins

Incubate for 5-9 days until spheroid formation is complete

B

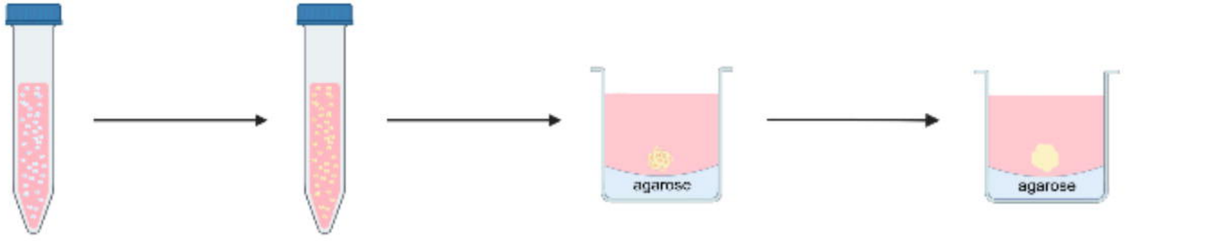


Passage HFF/MRC-5 cell culture. Suspend cells at a density of 1 x $10^6$ cells/mL

Dye-label the cells and suspend at a density of 1 x $10^5$ cells/mL

Add 100 µl of cell suspension to per well and centrifuge 340 *x g* for 10 mins

Incubate for 1-3 days until spheroid formation is complete

C

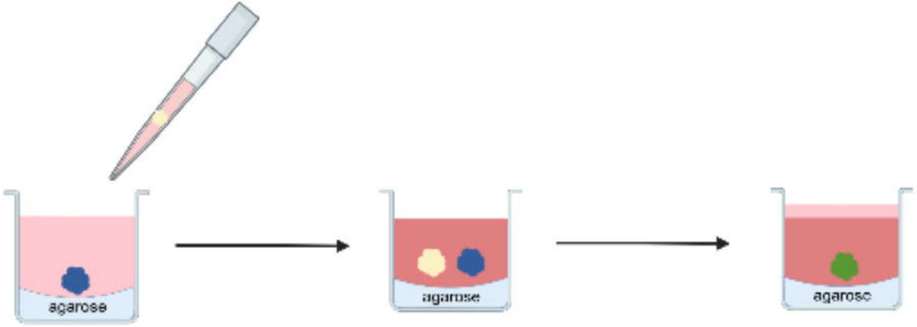


Transfer a single spheroid to a pre-existing well

Add matrix (MG or CG) at a 1:1-1:5 dilution and incubate for 3 hours

Add 75 µL of cDMEM and incubate for 2-3 days for assembloid formation

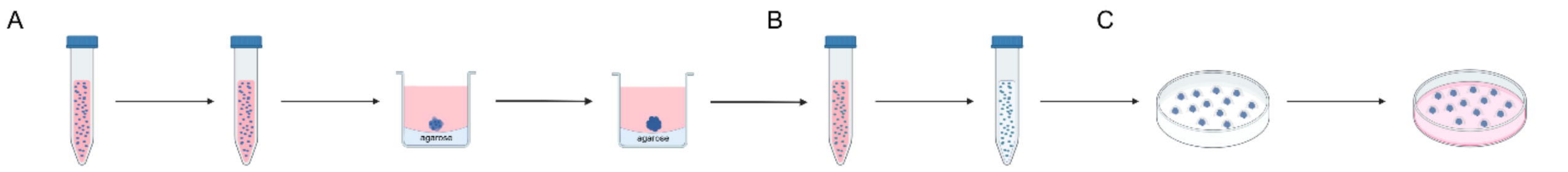
A
B
C
agarose
agarose
Passage HepG2-WT cell culture. Suspend cells at a density of 1 x 10⁵ cells/mL
Dye-label the cells and suspend at a density of 5 x 10⁴ cells/mL
Add 100 µl of cell suspension to per well and centrifuge 340 x g for 10 mins
Incubate for 5-9 days until spheroid formation is complete
Collect the HepG2-WT spheroids and gently rinse with cDMEM
Suspend the spheroids in matrix (MG or CG)
Seed one spheroid in 15 uL of matrix (MG or CG) onto 60 mm petri dish and incubate at 37°C
Slowly add 5 mL of growth medium and incubate at 37°C

A

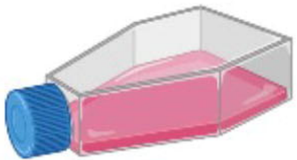

Seed 5,00 cells/cm$^2$ in 15 mL of cDMEM (T-75 flask)

72 hour incubation

Collect conditioned media and centrifuge at 290 *x g* for 5 mins

B

Filter conditioned media using a 0.2 µm syringe filter

Dilute conditioned media with cDMEM (1:1-1:7)

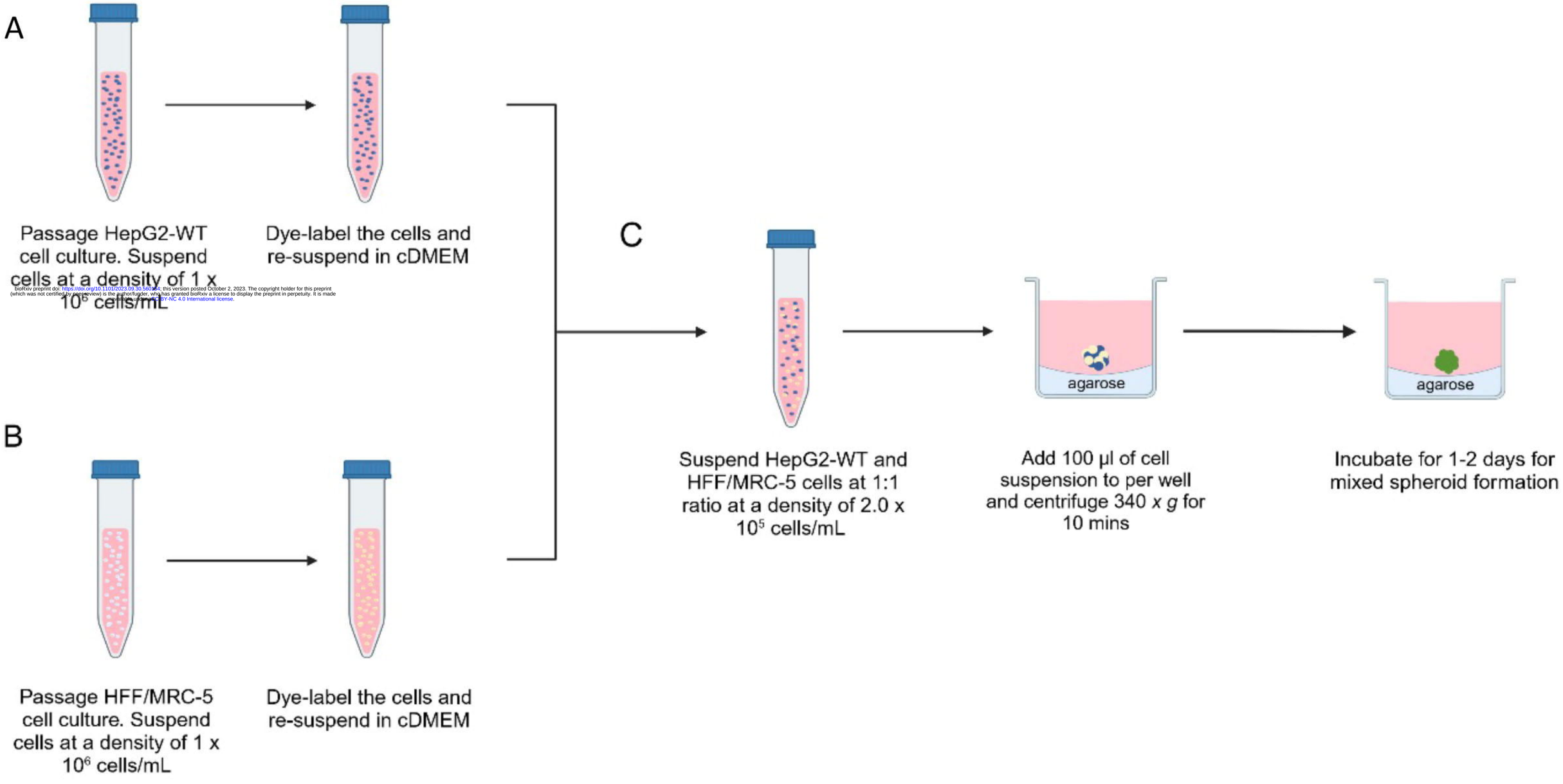

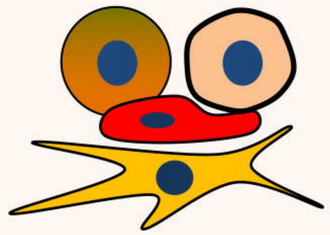

Self-organization

Collective migration

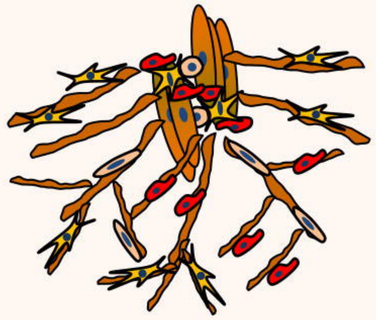

Branching morphogenesis

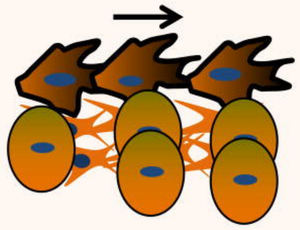

Interstitial migration

Synthetic tissues

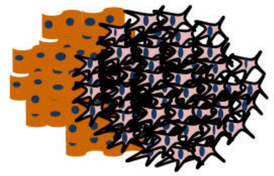

Organoid

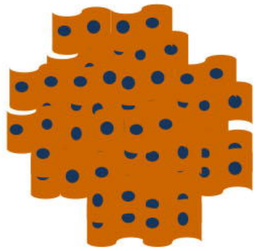

hPSC

*Morphogenesis/ Growth Toolbox*

Assembloid

Large Assembloid

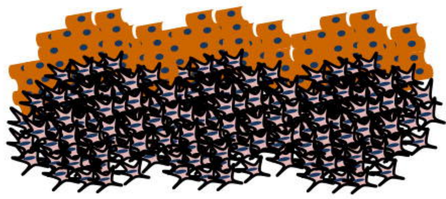



CELLS

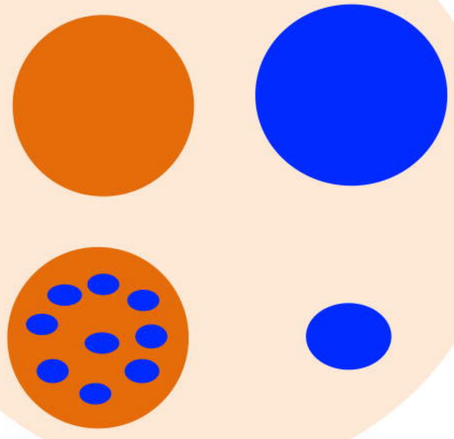

TOOLS

*Stiffness* *Microfluidics*

*Microfabrication* *Gene editing*

*Biomaterials* *Reprogramming*

BIOMATRIX

*Collagen* *Fibronectin*

*Matrigel* *Hydrogel*

*Fibrin* *Native ECM*

# HepG2-WT

Small (S)
1500 cells/well

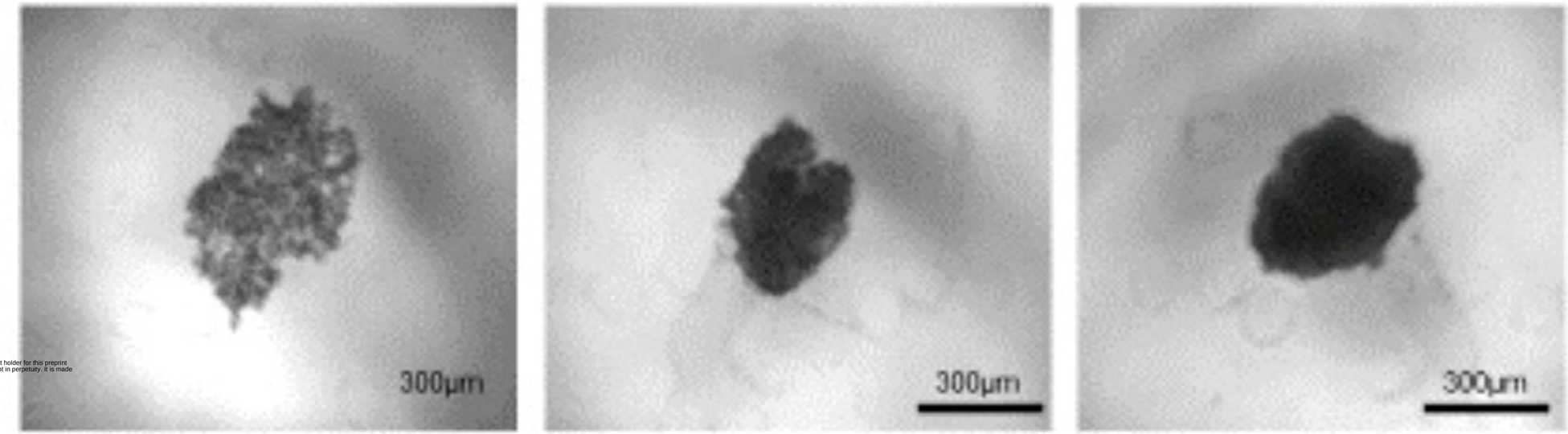


Large (L)
3000 cells/well

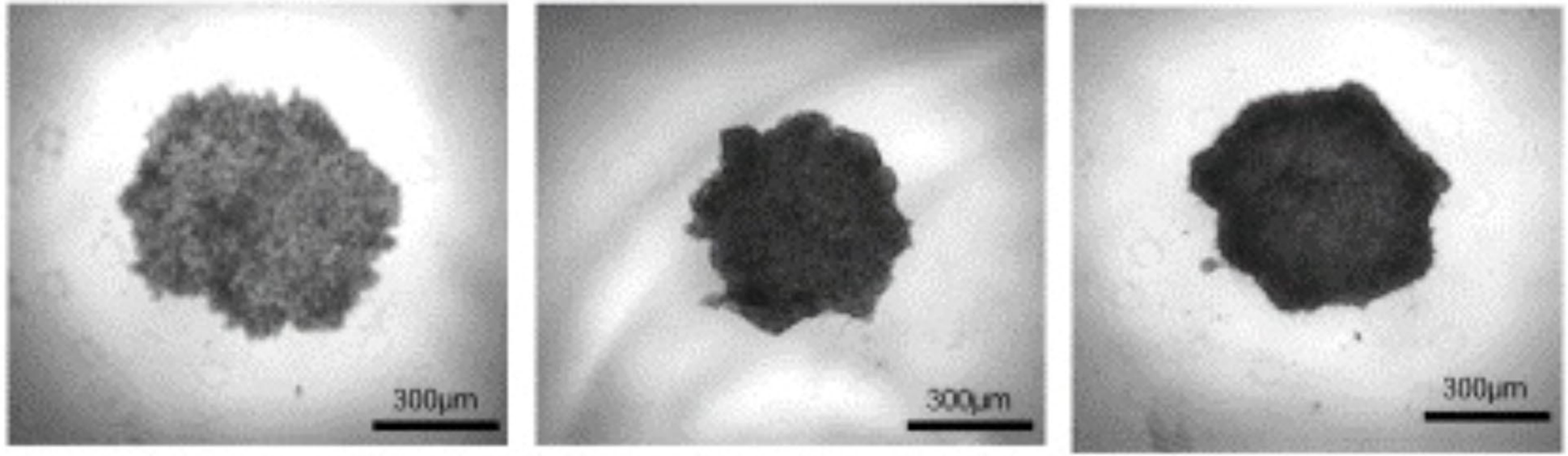


D1 D3 D5

Collagen + DMEM

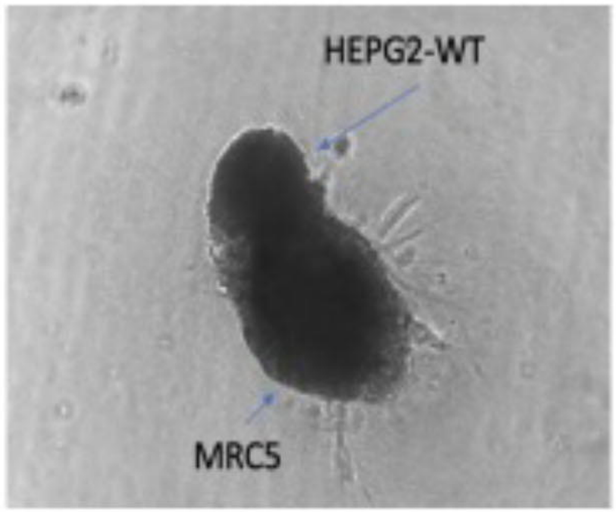


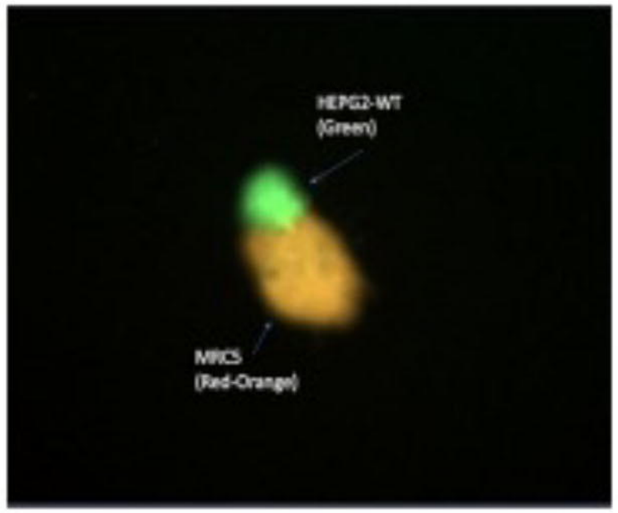


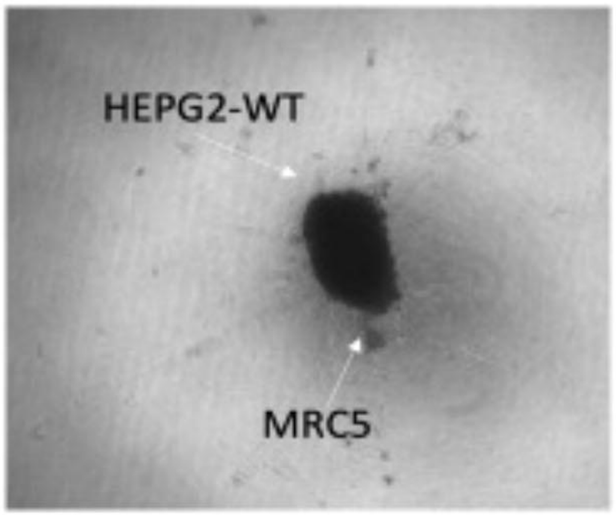


Collagen + MCM

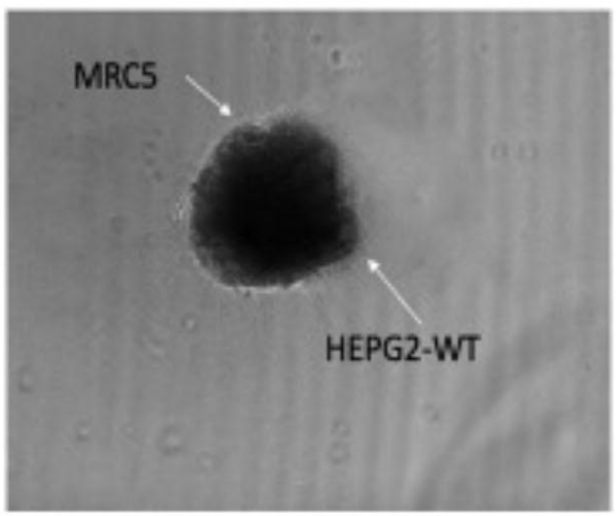


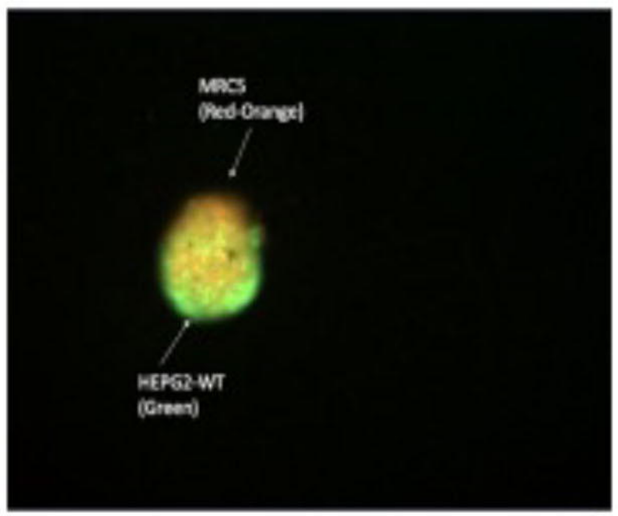


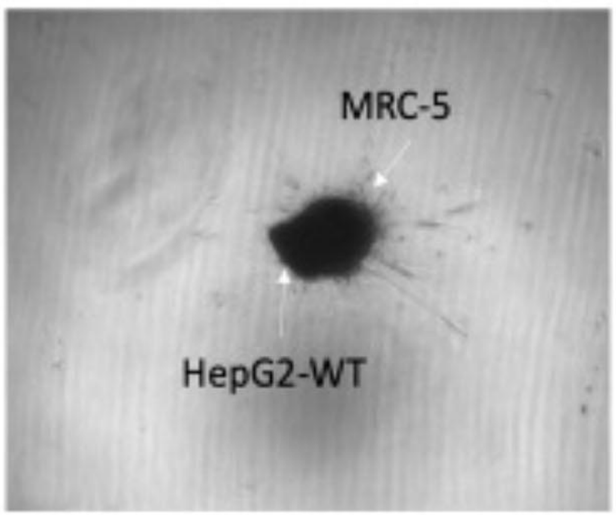


Matrigel + DMEM

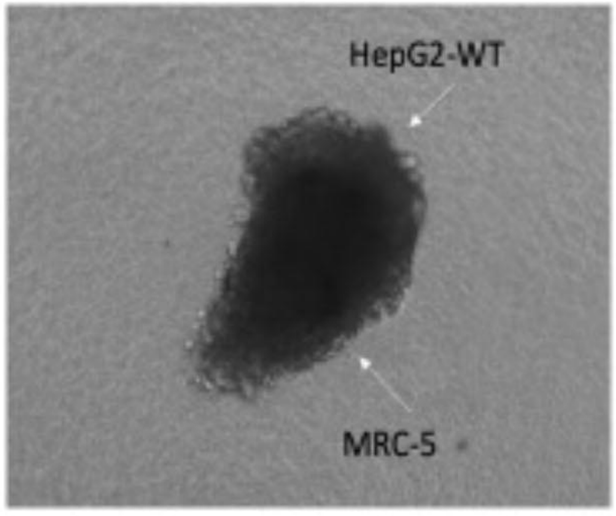


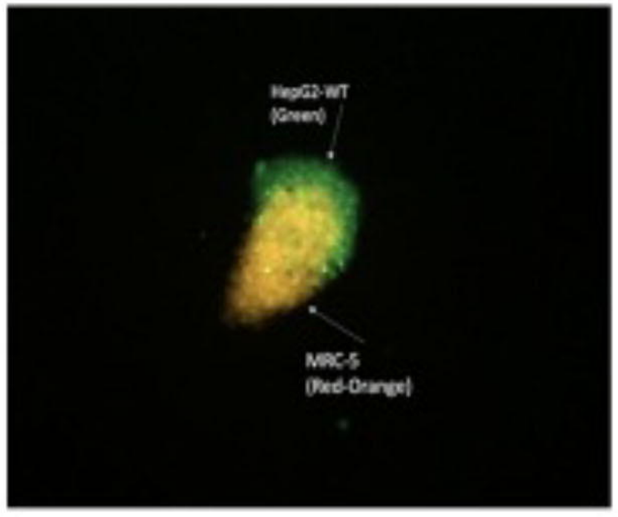


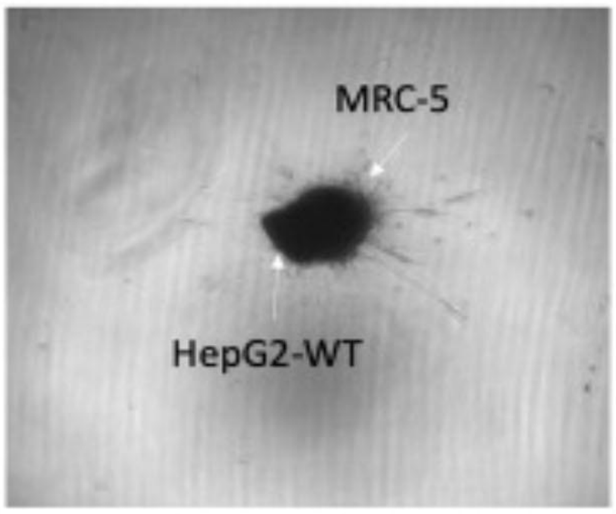


Matrigel + MCM

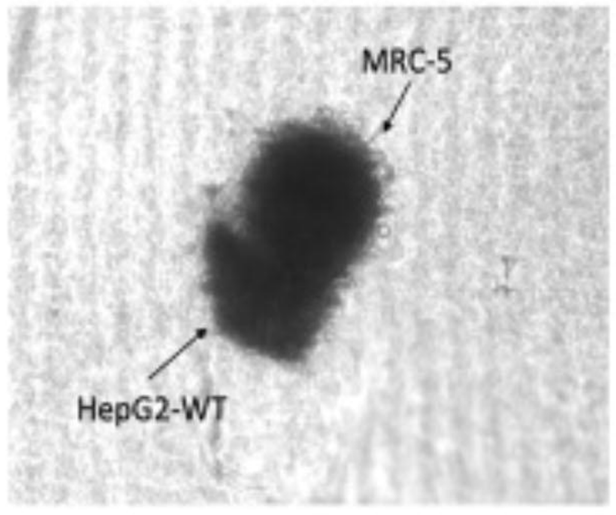


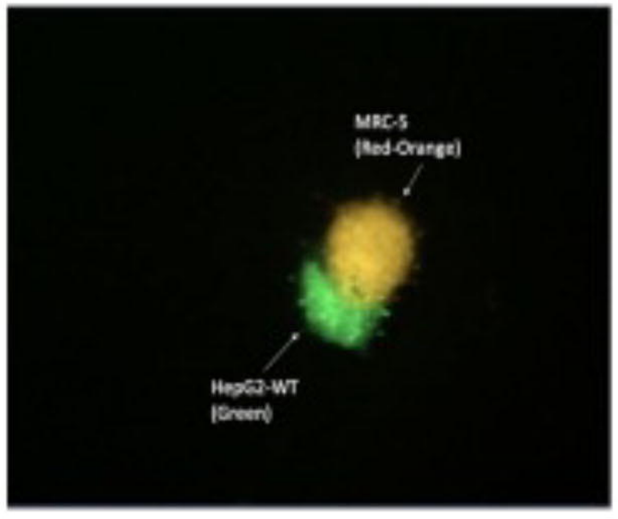


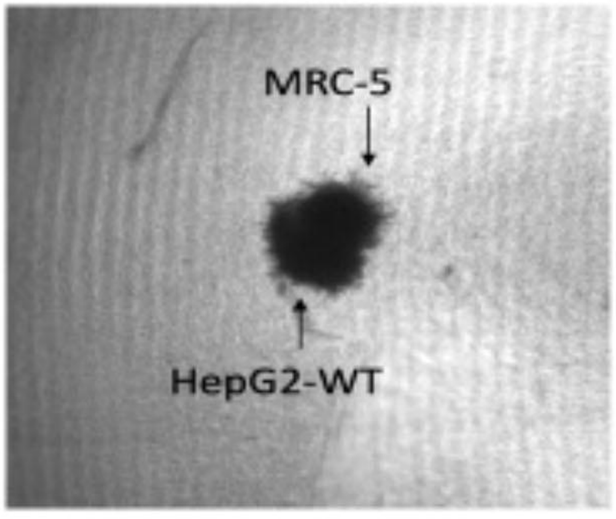


Day 2 | Day 2 (Dye labeled) | Day 4

A

## Building Large or Small Arms

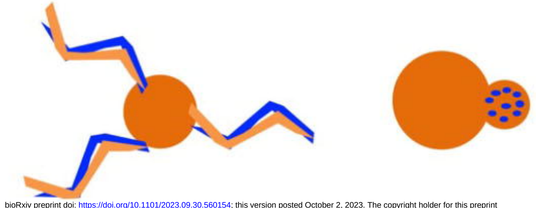

B

## HEP-MES Assembloids demonstrate branching arms

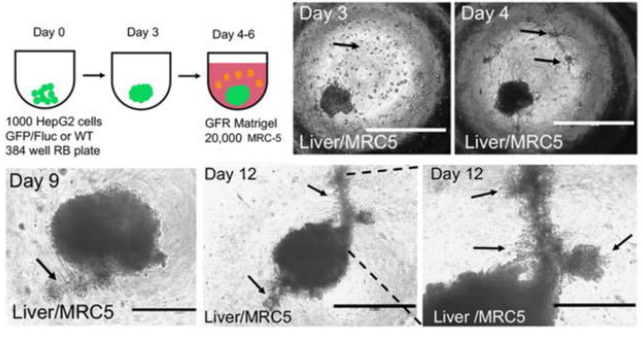


## Mixed spheroid form bridges with HEP spheroids

C

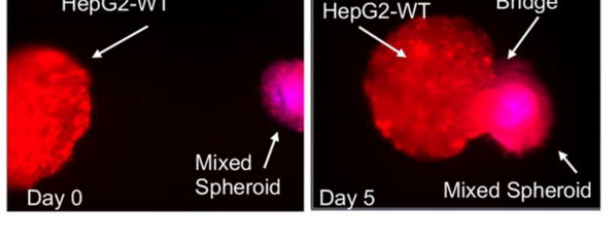


D

## Spot-Welding (fused edges)

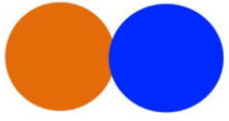

E

## HEP-MES in collagen with MES-conditioned medium fuse edges and don't form cupping

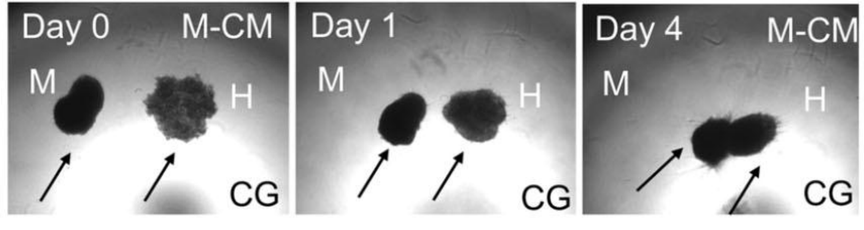


F

## In Collagen 2 mg/ml (stiff), HEP-MES edges fuse

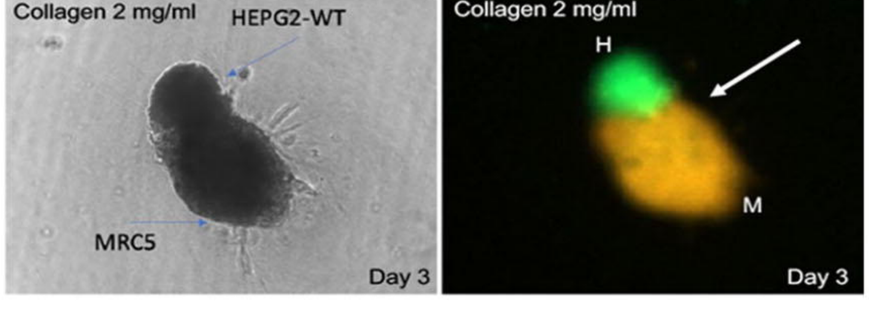


G

## Infiltrating and Layering

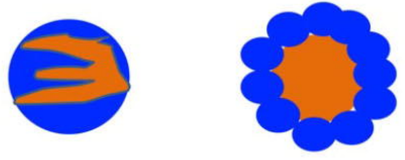

H

## HEP-MES infiltrate in Collagen, with MES- conditioned medium

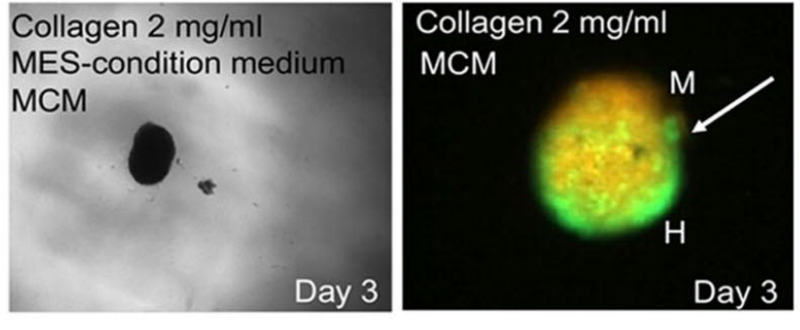


I

## HEP-inside, MES-outside leads to layered assembloid

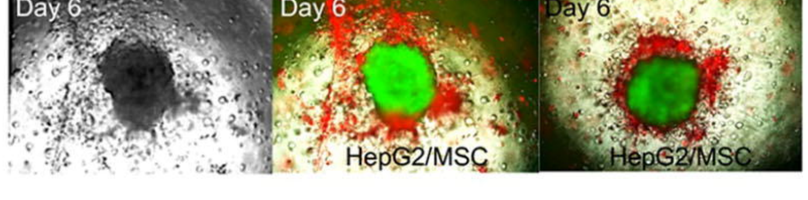

A

Fused HEP-MES assembloids (increased packing density, separate layers)

B

HEP and MES spheroids fuse in matrigel

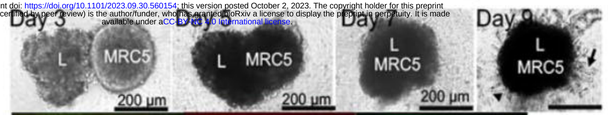


C

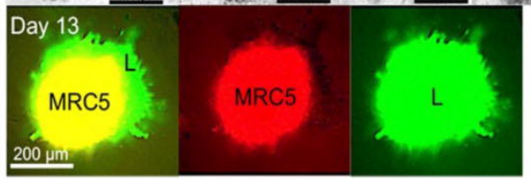


D

HEP-MES assembloids with multiple MES spheroids fuse but overall volume does not increase

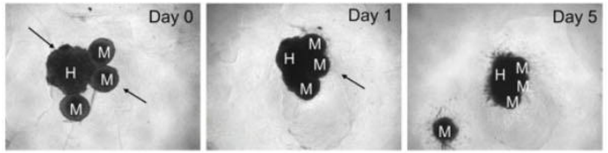


E

HEP-MES assembloids form under low serum

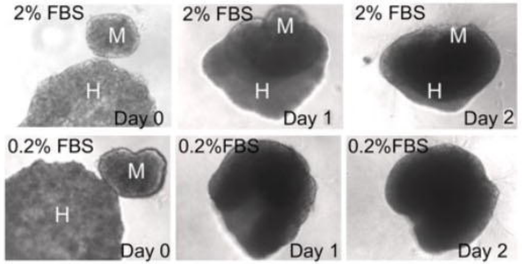


F

HEP-MES don't form at large distances in collagen with MES-conditioned medium

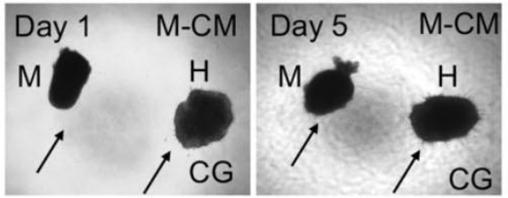


G

Mixed spheroids fuse with MES spheroids

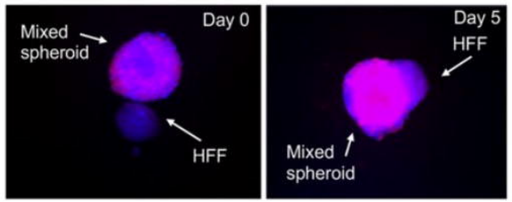


H

Cupping, partially fused HEP-MES assembloids (increased packing density, separate layers)

I

In collagen, HEP-MES form assembloids via cup-like mechanism

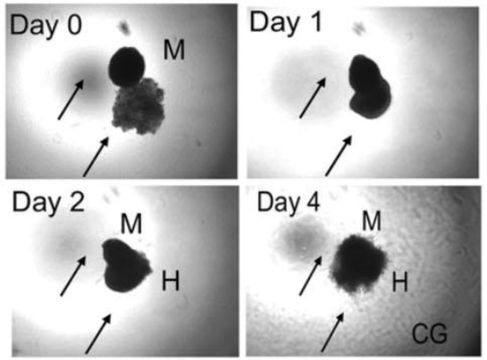


J

HEP-MES cupping prior to fusion in MG

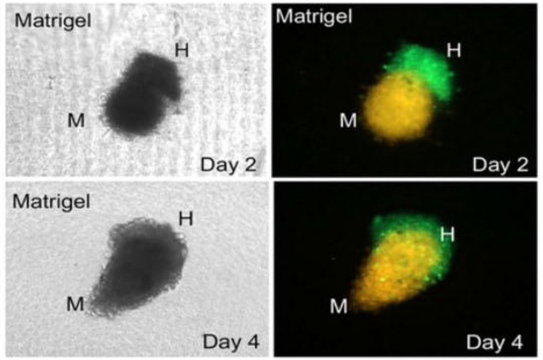


K

HEP-MES assembloids with multiple HEP spheroids combine with cupping mechanism

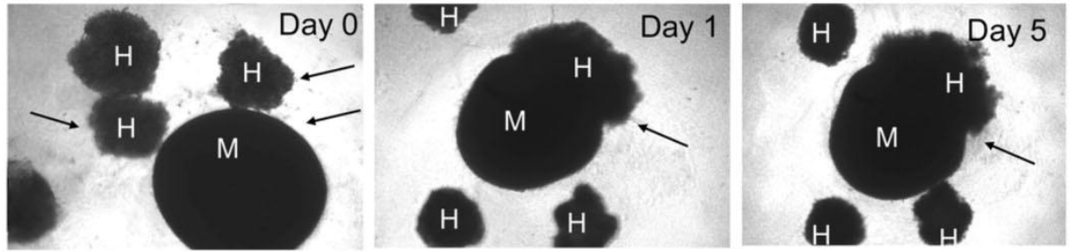

A

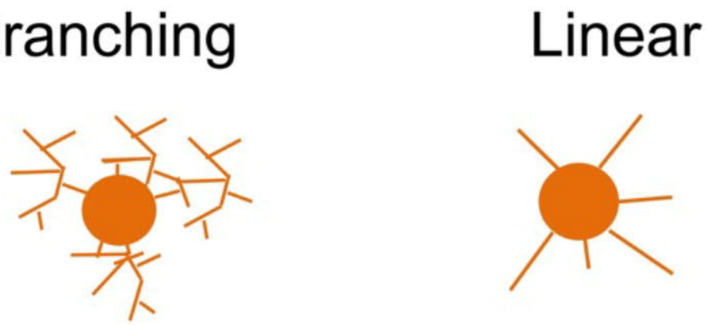


B

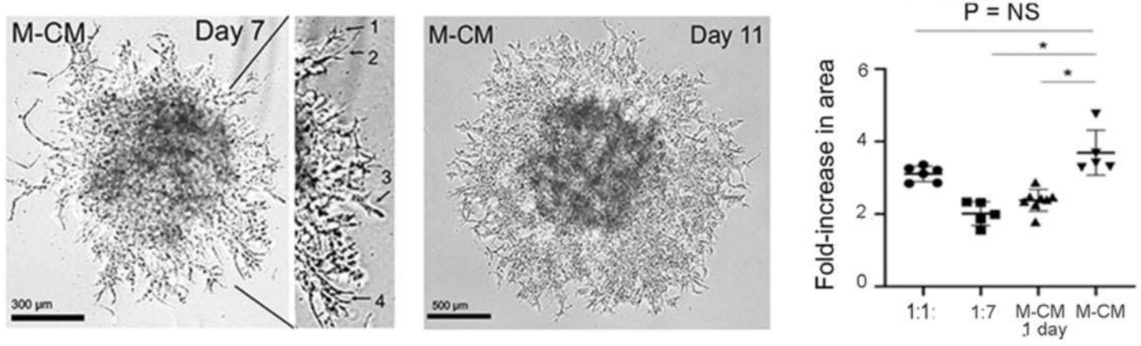


C

Branching morphogenesis of HEP-spheroids inhibited by TGF-beta

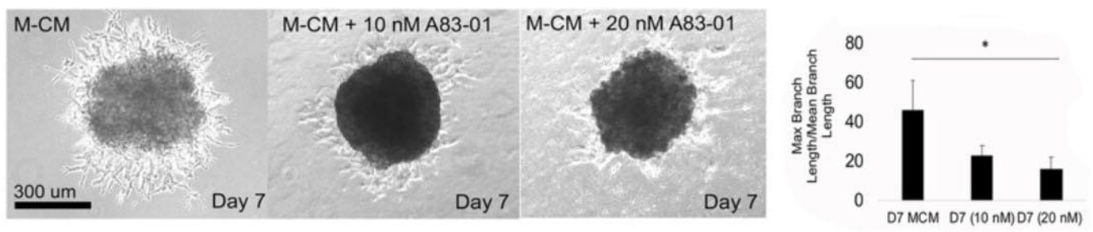


D

HEP spheroids demonstrate linear branching in collagen gels

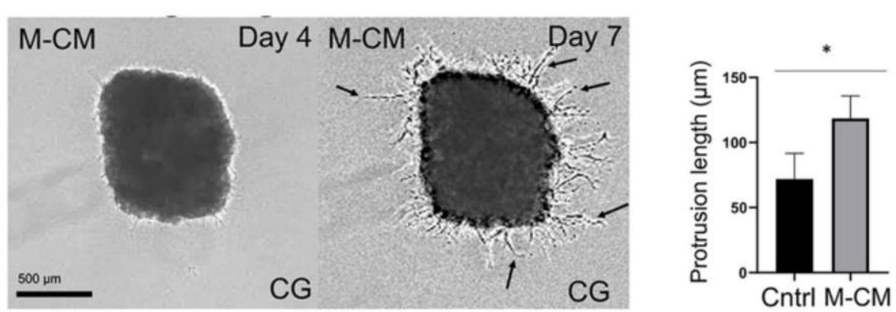


E

HEP-MES mixed spheroids demonstrate hair-like migration in Fibrin gels

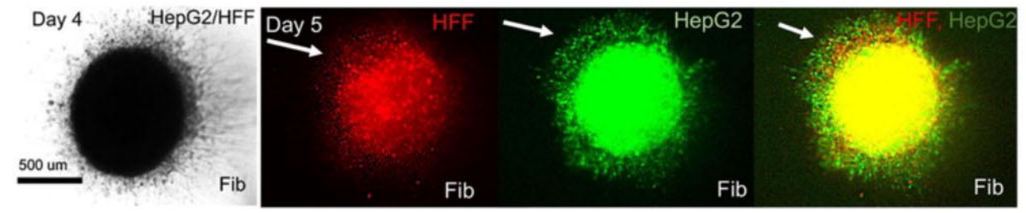


F

Star-shaped

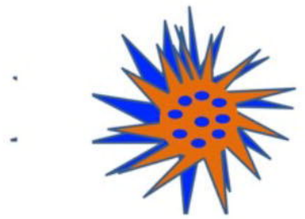

G

Increasing branch length in HEP-MES mixed spheroids with TGF-Beta

Tgfb + MRC5/ HepG2 in Matrigel

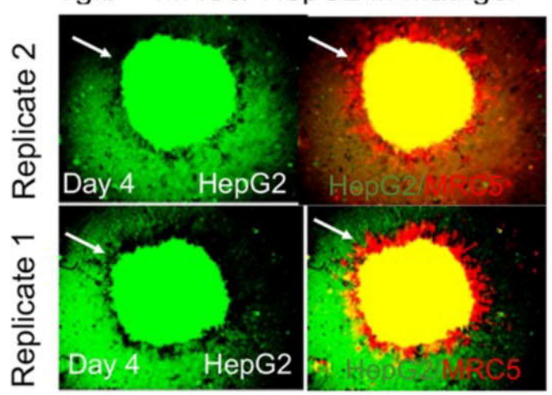


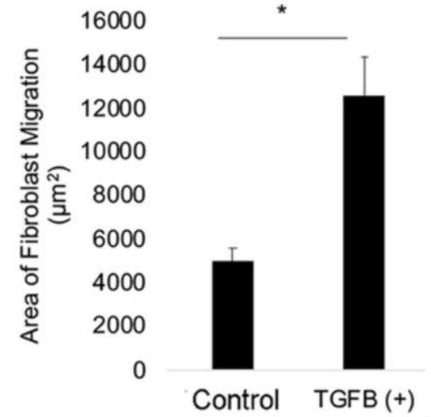

| Condition Media & Matrix | Initial Distances (μm) | Days to Merge |
|---|---|---|
| Matrigel + DMEM | 492.742 – 974.051 | 6-12 |
| Collagen + DMEM | 413.983 – 593.872 | 5-8 |
| Collagen + MCM | 695.235 | 9 |